Cancer Nanotechnology

DOI: 10.1002/anie.201209804

A Drug-Delivery Vehicle Combining the Targeting and Thermal Ablation of HER2+ Breast-Cancer Cells with Triggered Drug Release**

*Jin-Oh You, Peng Guo, and Debra T. Auguste**

Breast cancer is the second leading cause of cancer-related deaths in women, surpassed only by lung cancer.[1] Current clinical therapies target the estrogen receptor (ER) and human epidermal growth factor receptor-2 (HER2) to reduce cancer-cell proliferation. These methods are often used in conjunction with surgery, chemotherapy, and/or radiation in efforts to eradicate the disease. However, 25% of patients face tumor recurrence and resistance within 5 years after treatment.[2] Ideally, the initial treatment would supply a robust, broad-spectrum therapy to eliminate all cancer cells while minimizing damage to healthy tissue.

Tumor-targeting strategies have the potential to improve the therapeutic efficacy of chemotherapeutic agents relative to systemic approaches. To date, targeted therapeutics have been engineered by the use of receptor-mediated or stimuli-responsive methods. Molecules that recognize and/or inhibit receptor function—alone, pegylated, or tethered to a cargo—have been shown to improve targeting and reduce cancer-cell proliferation and/or migration (e.g., folate,[3] anti-CXCR4,[4] anti-HER2).[5] Stimuli-sensitive therapeutics have been used to direct delivery to the tumor site through activation by a physiological change or an external source; in this way, off-target effects were minimized. We previously synthesized a pH-sensitive drug-delivery vehicle that triggered the release of paclitaxel in acidic tumor environments.[6] The thermal ablation of tumors as a result of the localized heating of carbon nanotubes[7] or gold particles[8] activated with near-infrared (NIR) light was effective in the treatment of skin,[9] breast,[10] liver,[11] and ovarian cancers.[12] Individually, each targeted therapy provided a substantial advantage over nontargeted methods.

The integration of two targeting methods in one vehicle has improved tumoricidal efficacy relative to the use of each approach independently. A drawback associated with the merging of two targeting approaches is the introduction of additional synthesis and purification steps, which often lead to low encapsulation of the drug. Doxorubicin (Dox) encapsulation can reduce the overall efficacy of the chemotherapeutic agent relative to systemic administration.[13] Dox, an effective and widely used chemotherapeutic agent owing to its hydrophilicity and high toxicity, suffers from low drug loading and fast release rates when encapsulated within polymeric nanoparticles. Furthermore, the simultaneous or stepwise delivery of heat and the drug may drastically affect the therapeutic result.[14] A tunable drug-delivery strategy engineered to provide the greatest therapeutic impact would be desirable.

In this study, we synthesized a single drug carrier that targets HER2, triggers Dox release, and thermally ablates breast-cancer cells. The particles encapsulate Dox within a pH-sensitive matrix that is embedded with Au nanoparticles and decorated with poly(ethylene glycol)–HER2 conjugates within five steps (Figure 1; PEG = poly(ethylene glycol)). Dithiolated dimethylaminoethyl methacrylate (dT-DMAEMA), the pH-responsive monomer, was synthesized by reversible addition–fragmentation chain-transfer (RAFT) polymerization and characterized by NMR spectroscopy (see Figure S1 in the Supporting Information). Particles encapsulating Dox were prepared by oil-in-water emulsification. Tuning of the dT-DMAEMA/HEMA ratio and the pH value of the buffer regulated the swelling properties of the matrix. We have previously shown that DMAEMA/HEMA matrices are sensitive to incremental changes in the pH value (>0.2 pH units).[6,15] The pH-responsive matrix effectively acts as a logic gate: Dox is entrapped within the matrix until the network is opened.

Subsequently, gold nanoparticles were formed homogeneously throughout the pH-responsive matrix. Thiol groups in dT-DMAEMA show affinity for colloidal Au and Au ions. dT-

[*] Prof. Dr. J.-O. You, Dr. P. Guo, Prof. Dr. D. T. Auguste
School of Engineering and Applied Sciences, Harvard University, Cambridge, MA 02138 (USA)
Prof. Dr. J.-O. You
Department of Engineering Chemistry, Chungbuk National University, Cheongju, 361-763 (Republic of Korea)
Dr. P. Guo, Prof. Dr. D. T. Auguste
Department of Surgery, Harvard Medical School
Boston, MA 02115 (USA)
and
Vascular Biology Program, Children's Hospital Boston
Boston, MA 02115 (USA)
and
Department of Biomedical Engineering, The City College of New York, New York, NY 10031 (USA)
E-mail: dauguste@ccny.cuny.edu

[**] We thank Prof. David Mooney and Dr. Praveen Arany for use of the NIR laser device and Dariela Almeda for FACS analysis. We gratefully acknowledge financial support from the Kavli Institute for Bionano Science and Technology at Harvard University. This research was supported by NIH (1DP2A174495) and NSF (DMR-0820484). This research was performed in part at the Center for Nanoscale Systems (CNS), a member of the National Nanotechnology Infrastructure Network (NNIN), which is supported by the National Science Foundation under NSF award no. ECS-0335765. CNS is part of the Faculty of Arts and Sciences at Harvard University.

Supporting information for this article is available on the WWW under http://dx.doi.org/10.1002/anie.201209804.

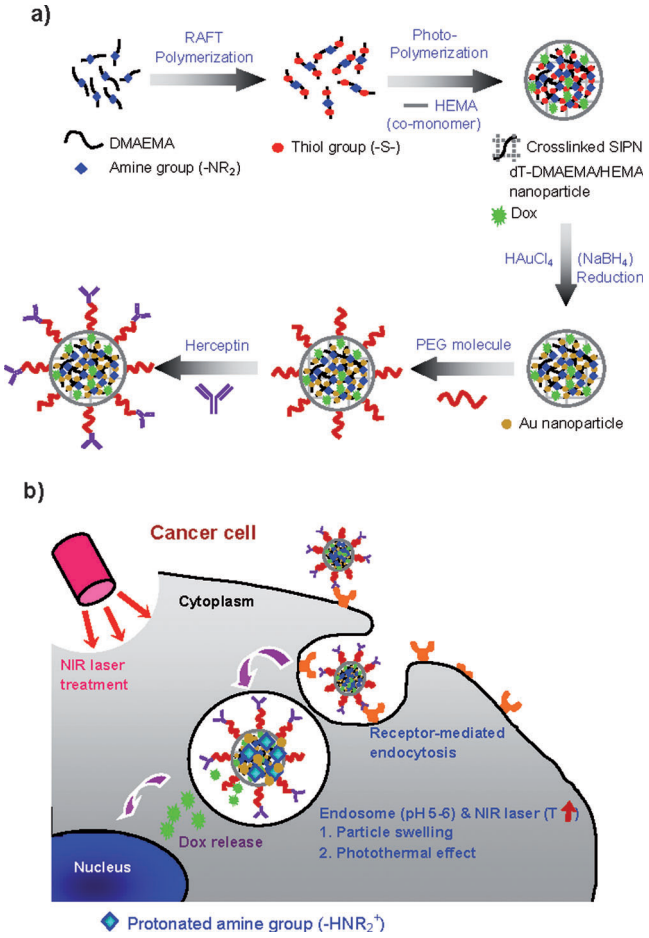

Figure 1. Schematic diagrams of a) the synthesis of Herceptin-conjugated, Dox-encapsulating, and pH-sensitive dT-DMAEMA/HEMA (HPG-Dox-30D70H) nanoparticles and b) cancer therapy. SIPN = semi-interpenetrating polymer network.

DMAEMA/HEMA nanoparticles were immersed in an aqueous solution of potassium tetrachloroaurate ($KAuCl_4$) and reduced with a solution of sodium borohydride ($NaBH_4$).[16] Au nanoparticles were distributed homogeneously within the Dox-encapsulating dT-DMAEMA/HEMA nanoparticles (30:70 (mol/mol); Figure 2a). This transformation was also observed visually; the white particles became brown after Au synthesis (Figure 2a i,ii).

The particles were functionalized on the exterior with difunctional poly(ethylene glycol) molecules (SH-PEG-COOH, 10 μmol/10 mg particles) substituted with a thiol group at one end and a carboxylic acid group at the other. The introduction of a thiol group enabled the noncovalent attachment of PEG to Au and dT-DMAEMA. Thiol-functionalized PEGs are useful for triggering the release of PEG within the glutathione-rich cytoplasmic environment.[17] After the separation of anchored PEG from free PEG in solution by dialysis, Herceptin was conjugated through a carbodiimide reaction (9 nmol/10 mg particles). Herceptin has been shown clinically to target and reduce proliferation in HER2+ breast tumors.[18] Herceptin–PEG-labeled, gold-embedded, Dox-encapsulating, pH-responsive 30 dT-DMAEMA/70 HEMA (mol/mol) nanoparticles (HPG-Dox-30D70H) were designed to target HER2+ breast-cancer cells, trigger the release of Dox, and induce hyperthermia upon activation by irradiation with a near-infrared (NIR) laser.

The size and morphology of all nanoparticles were examined by transmission electron microscopy (TEM; Figure 2a) and dynamic light scattering (see Table S1 in the Supporting Information). Examination of the nanoparticles revealed a uniform and smooth surface morphology (see Figure S2a). The average diameter of HPG-Dox-30D70H nanoparticles was (186.4 ± 18.6) nm (see Figure S2b) with a negative surface charge of −7.3 ± 2.1 mV. The size and charge of HPG-Dox-30D70H are suitable for systemic delivery; these nanocarrier traits have resulted in enhanced permeability and retention (EPR).[19] The negative charge of HPG-Dox-30D70H is caused by unreacted PEG-COOH. The amine groups in DMAEMA become protonated as the pH value decreases. As the dT-DMAEMA content increased from 10 to 30%, the ζ potential rose from −18.9 to −7.3 mV in parallel. Nanoparticle aggregation in a serum-free medium was not observed during cell-viability and targeting experiments.

The Au content of HPG-Dox-10D90H (10 dT-DMAEMA/90 HEMA (mol/mol)) and HPG-Dox-30D70H was characterized by thermogravimetric analysis (TGA) by heating from 20 to 600 °C under a continuous flow of argon (Figure 2b). TGA analysis of the Au-embedded, pH-sensitive nanoparticles revealed an Au-nanoparticle content of (1.45 ± 0.10) and (2.71 ± 0.22) % (w/w) for HPG-Dox-10D90H and HPG-Dox-30D70H, respectively. The Au density increased with the Au content of the dT-DMAEMA particles. In a previous study, we demonstrated that under similar reaction conditions the in situ synthesis of Au colloids was dictated by the initial thiol content.[16b] The encapsulation of Dox had no effect on the ability to synthesize Au colloids within dT-DMAEMA/HEMA matrices. The UV/Vis spectrum of HPG-Dox-30D70H nanoparticles indicated absorption in the near-infrared range with a peak at 795 nm (Figure 2c).

To demonstrate the potential of HPG-Dox-30D70H for photothermal cancer therapy, we exposed HPG-Dox-30D70H nanoparticles to NIR laser irradiation at 810 nm with a power density of 5 $W cm^{-2}$ for 10 min. Changes in temperature were measured and imaged by a thermal camera over the duration of the experiment (Figure 2d i,ii). Representative thermal images taken at different time points during the exposure of HPG-Dox-30D70H (5 $mg mL^{-1}$) to NIR irradiation show the temperature distribution within each well (see Figure S3). The temperature of HPG-Dox-30D70H aqueous solution increased by 15.3 °C during this experiment; under the same conditions, the temperature of nanoparticle-free distilled water increased by almost 1 °C. During NIR laser irradiation, the particle size was not affected by changes in temperature.

In addition to local heating, the nanocarriers were designed to swell in response to changes in the pH value, and thus to trigger the release of Dox. Volumetric swelling was measured as a function of the molar ratio of dT-DMAEMA to HEMA and of the pH value of the swelling medium (Figure 2e,f, respectively). The volume swelling ratio

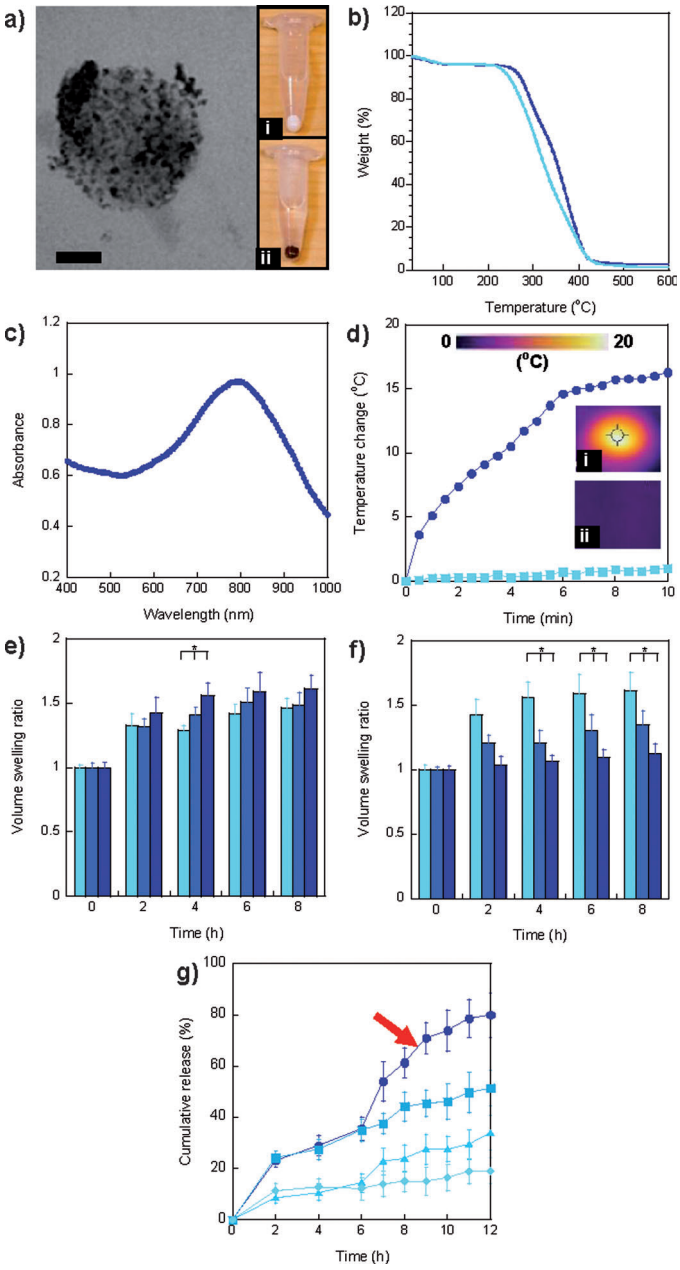

Figure 2. Characterization of multitargeted nanoparticles. a) TEM image of an HPG-Dox-30D70H nanoparticle. Au nanoparticles were homogeneously distributed in the nanoparticles. Images were taken of the nanoparticle pellets after the centrifugation of Dox-30D70H (white, i) and HPG-Dox-30D70H (dark brown, ii). Scale bar: 50 nm. b) TGA curves of HPG-Dox-10D90H (light blue) and HPG-Dox-30D70H (dark blue). c) UV/Vis spectrum of HPG-Dox-30D70H nanoparticles (peak at 795 nm). d) Temperature change of HPG-Dox-30D70H in distilled water (5 mg mL^{-1}; dark blue) and nanoparticle-free distilled water (light blue) during NIR laser irradiation for 10 min. Images were taken with an NIR thermal camera for i) HPG-Dox-30D70H in distilled water and ii) only distilled water after NIR laser irradiation for 10 min. e) Volume swelling ratios of HPG-Dox-10D90H (light blue), HPG-Dox-20D80H (blue), and HPG-Dox-30D70H (dark blue) in 20 mM phosphate buffer (pH 5.5) at 0, 2, 4, 6, and 8 h. f) Volume swelling ratios of HPG-Dox-30D70H in 20 mM phosphate buffer at pH 5.5 (light blue), 6.5 (blue), and 7.4 (dark blue) at 0, 2, 4, 6, and 8 h. g) Cumulative Dox release from HPG-Dox-30D70H (5 mg mL^{-1}) in 20 mM phosphate buffer at pH 5.5 (squares, dark-blue curve) and 7.4 (diamonds, light-blue curve) over 12 h. To evaluate the photothermal effect induced by NIR irradiation, HPG-Dox-30D70H was incubated at pH 5.5 (circles) and 7.4 (triangles) in 20 mM phosphate buffer and then irradiated with an NIR laser for 6 h. The error is the standard deviation from the mean ($n = 3$, * is $P < 0.05$).

is defined as the nanoparticle diameter after swelling divided by the original diameter.[20] Figure 2e depicts the swelling ratio for dT-DMAEMA/HEMA molar ratios of 10:90, 20:80, and 30:70 as a function of time. The swelling ratio of dT-DMAEMA/HEMA nanoparticles increased with the dT-DMAEMA content owing to the greater number of protonated amine groups. After 4 h at pH 5.5, the swelling ratio of HPG-Dox-10D90H and HPG-Dox-30D70H had increased to 1.29 ± 0.04 and 1.56 ± 0.09, respectively. To investigate the pH sensitivity of the nanoparticles, we measured the swelling ratio of HPG-Dox-30D70H as a function of the pH value (Figure 2f). The swelling ratios (measured after 8 h) increased from 1.13 ± 0.07 at pH 7.4 to 1.61 ± 0.14 at pH 5.5. The nanoparticle formulation may be tuned to control pH-induced swelling.

Dox was encapsulated during particle synthesis. The efficiencies of Dox encapsulation in HP-Dox-30D70H (without gold) and HPG-Dox-30D70H nanoparticles were (95.2 ± 3.1) and (72.3 ± 6.7)%. The reduction in Dox loading was a result of multiple washing steps after Au synthesis and antibody conjugation. Dox encapsulation is high within liposome formulation (greater than 90%);[21] polymeric nanoparticles have failed to show similar results.[22]

To confirm that pH-induced swelling triggered the release of Dox, Dox release was measured as a function of time at pH 5.5 and 7.4 (Figure 2g). The release of Dox was significantly enhanced under acidic conditions. After 8 h, (44.05 ± 5.79)% of the encapsulated Dox had been released at pH 5.5, whereas (15.01 ± 3.80)% had been released at pH 7.4. In comparison, for other pH-sensitive nanocarriers, 25% Dox release after 24 h at pH 5.5 was reported,[23] or a significant burst release (50% of the loaded Dox) was observed.[13b] Our pH-sensitive nanocarriers exhibited a slow, controlled release of Dox at pH 7.4 and then a rapid release upon a decrease in the pH value.

We also investigated the ability of HPG-Dox-30D70H nanoparticles to release Dox under NIR laser irradiation. HPG-Dox-30D70H nanoparticles were allowed to release Dox in a buffer at pH 5.5 for 6 h and then heated (810 nm, 5 W cm^{-2}, 6 h). Dox release was enhanced at pH 5.5 after laser irradiation relative to that observed for the nonirradiated control (Figure 2g). The temperature of the well increased from 37.7 to 48.9 °C after NIR irradiation for 5 min, which significantly increased Dox release (see Figure S3). Approximately 30% of the initial dose was delivered when the pH value changed; subsequent irradiation delivered an additional 50% of the entrapped drug. At pH 7.4, only 10% of the

initial dose was available after 6 h; this amount increased to 30% of the entrapped drug after laser irradiation. The coupling of pH-triggered release and localized heating in one carrier yielded enhanced Dox delivery. This synergistic delivery approach enables the tunable release of Dox within the tumor microenvironment.

The HPG-Dox-30D70H nanoparticles were conjugated with Herceptin for the targeting of HER2+ breast-cancer cells. The number of Herceptin molecules on the nanoparticle surface was determined by a DC (detergent-compatible) protein assay (see Table S2). Approximately 116 and 117 Herceptin molecules were conjugated on HPG-30D70H and HPG-Dox-30D70H nanoparticles, respectively. The binding affinity of HPG-Dox-30D70H for a breast-cancer cell line with low HER2 expression, MCF-7, and a breast-cancer cell line that overexpresses HER2, SK-BR-3, was measured by flow cytometry (Figure 3). As a control, IgG–PEG-labeled

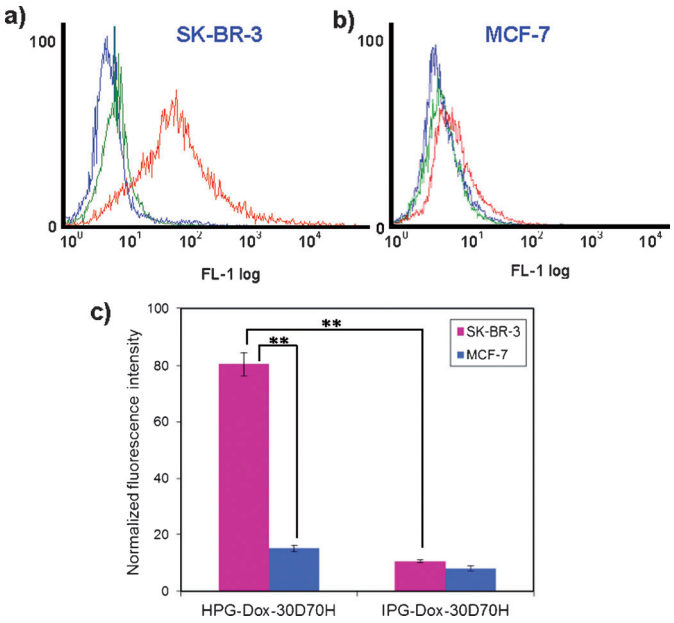

Figure 3. a,b) Flow cytometry analysis of SK-BR-3 (a) and MCF-7 (b) cells treated with HPG-Dox-30D70H or IPG-Dox-30D70H. The blue, green, and red curves correspond to nontreated, IPG-Dox-30D70H-treated, and HPG-Dox-30D70H-treated samples, respectively. c) Normalized fluorescence intensities determined by flow cytometry. The error is the standard deviation from the mean ($n=3$, ** is $P<0.001$).

(IgG = immunoglobulin G), gold-embedded, Dox-encapsulating, pH-responsive, 30 dT-DMAEMA/70 HEMA nanoparticles (IPG-Dox-30D70H) were prepared. As expected, HPG-Dox-30D70H nanoparticles exhibited a 5.4-fold enhancement in the binding of SK-BR-3 cells relative to the binding of MCF-7 cells. These results confirmed claims in previous reports that Herceptin may be used to distinguish between cell lines with low and high HER2 expression.[24] Our HPG-Dox-30D70H nanocarriers exhibited similar behavior to that described in prior reports of HER2 targeting.[22]

To investigate the therapeutic efficacy of HPG-Dox-30D70H, we treated SK-BR-3 and MCF-7 cells with HPG-Dox-30D70H with and without laser irradiation (at a concentration equivalent to 0.26 μM Dox). This dose was 10-fold lower than the half maximal inhibitory concentration (IC_{50}) for free Dox (see Figure S4). Nontargeting IPG-Dox-30D70H was used as a control. Cell viability was measured quantitatively by a fluorescence plate reader and qualitatively by microscopy. SK-BR-3 cells treated with HPG-30D70H (without Dox) and HPG-Dox-30D70H without laser irradiation at pH 7.4 exhibited (77.31 ± 4.13) and (51.81 ± 5.39)% cell viability, respectively. After NIR laser irradiation, SK-BR-3 cell viability significantly decreased to (31.23 ± 7.68) and (14.49 ± 3.60)% for HPG-30D70H and HPG-Dox-30D70H, respectively. HPG-Dox-30D70H (Figure 4c,d) showed an enhanced tumoricidal effect relative to the antibody-labeled nanoparticle without Dox, HPG-30D70H (Figure 4a,b). When laser irradiation was added, the tumoricidal effect was enhanced by both the increased temperature and Dox release. The treatment of SK-BR-3 cells with nanoparticles that coupled receptor targeting, chemotherapy, and thermal ablation resulted in a maximal cell survival of 14%. Given the low Dox concentration and mild irradiation conditions, this level of toxicity is significantly more efficacious than the use of systemic Dox or combinations of Herceptin/Dox, Herceptin/NIR, or Dox/NIR.

Conversely, no significant difference was observed between HPG-30D70H and HPG-Dox-30D70H in their effect on MCF-7 cells in the absence of NIR laser irradiation. After exposure to NIR laser irradiation, the cell viability of MCF-7 cells treated with HPG-30D70H (Figure 4e,f) and HPG-Dox-30D70H (Figure 4g,h) was not significantly different. This result is attributed to lack of targeting, the low dose, and reduced Dox release.

IPG-30D70H and IPG-Dox-30D70H were used as controls for the cell-toxicity experiments. With these nanoparticles, the tumoricidal effect was hindered as a result of nonspecific targeting (Figure 4i,j; see also the fluorescence images in Figure S5). The nanocarriers without Dox were not cytotoxic (approximately 91–93% cell viability for both cell lines with and without Au synthesis). The viability results were similar to those found with poly(lactic-co-glyoclide) (PLGA) nanoparticles (nearly 93% for both cell lines), which are widely used for systemic drug delivery (see Figure S6).

Other "multifunctional" vehicles have incorporated two modalities, either Dox/NIR,[25] Dox/targeting,[26] or targeting/NIR.[22] Significantly better results were reported for these systems than for the unidimensional control with either Dox, NIR irradiation, or the targeting moiety alone. Ideally, Dox delivery would be localized to avoid off-target effects, and Dox would be released quickly. Dox-encapsulating PLGA nanoparticles exhibit slow release.[27] Stimuli-triggered delivery could be beneficial. However, previous examples of pH sensitivity exhibited either slow release or an uncontrolled burst release.[28] The vehicles presented herein are different: they have a high encapsulation efficiency and can trigger Dox release within hours in response to a small change in the pH value.

The functionalization of particles with an antibody or peptide is a conventional approach for targeting. Nanocarriers that couple both a targeting moiety and either Au

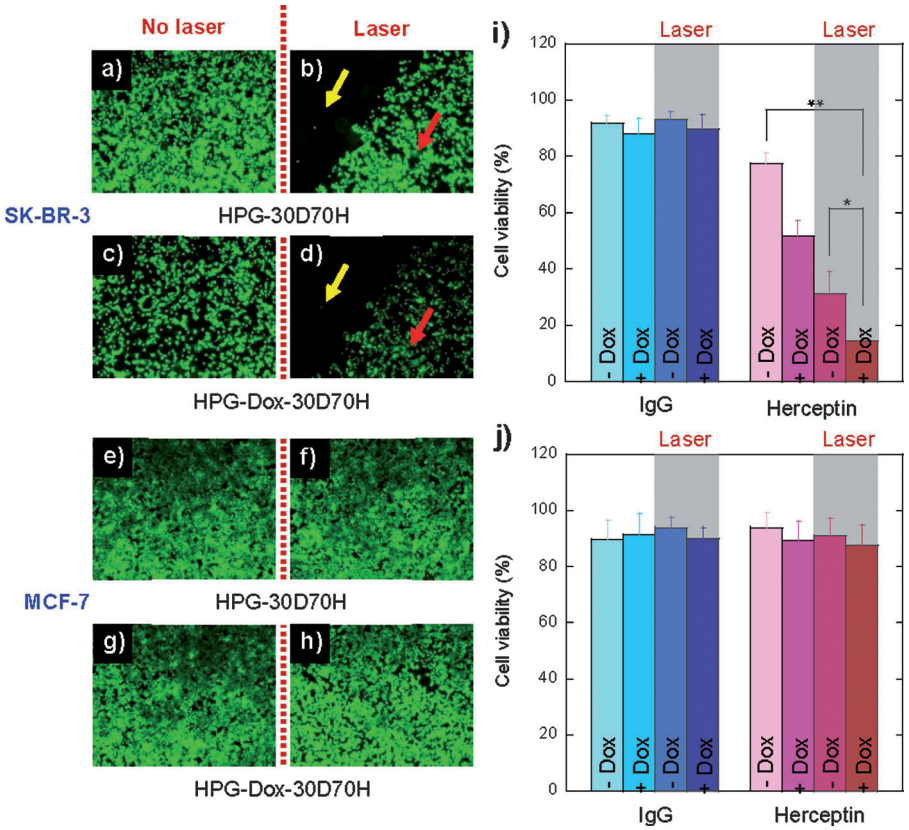

Figure 4. a–h) Fluorescence microscopy images of SK-BR-3 (a–d) and MCF-7 (e–h) cells treated with HPG-30D70H and HPG-Dox-30D70H with or without NIR laser illumination. Multitargeted nanocarriers were conjugated with Herceptin (a–h) or IgG (see Figure S3c-l in the Supporting Information). Yellow and red arrows indicate the areas treated and not treated with the NIR laser, respectively. i,j) The cell viability of SK-BR-3 (i) and MCF-7 (j) cells was determined by a resazurin-based toxicology assay. Cells were treated with nanocarriers conjugated with either Herceptin or IgG. The error is the standard deviation from the mean ($n=3$, * is $p<0.05$, ** is $P<0.01$).

nanoparticles[22] or Dox[26] on the surface show a significant decline in targeting ability. We chose Herceptin because it was currently used in the clinic. Herceptin-functionalized nanoparticles (HPG-30D/70H) without Dox or laser irradiation resulted in 77% cell viability. The presence of Herceptin alone did not result in a significant tumoricidal effect. Targeting with the addition of encapsulated Dox has been shown to be useful; however, we have demonstrated that some cancer-cell types are resistant to this type of therapy and require the use of alternative methods.[29]

Laser irradiation is a powerful technique that can achieve penetration depths of up to 50 mm.[30] HPG-30D/70H nanoparticles exhibited 30% cell viability after laser irradiation. Cancer cells were reported to be most vulnerable to hyperthermia and chemotherapeutic agents above 43 °C.[14] In this study, we used mild irradiation conditions (810 nm, 10 min, 5 W cm^{-2}) to cause a temperature increase of 15 °C, whereas an increased laser power was required in other studies for similar results (10 min, 15 W cm^{-2};[22] 3 min, 32 W cm^{-2};[31] 7 min, 80 W cm^{-2}).[32]

Our multitargeted nanoparticles have gold nanoparticles embedded homogeneously throughout the matrix. For many drug-delivery vehicles that induce local heating upon NIR irradiation, gold surface coatings are used.[22] Instead, in our method, we employed polymers as a template for Au colloids. We have demonstrated that the NIR thermal effect on Au nanoparticles is similar to that observed with Au coatings (Figure 2d). Additionally, our templating method is suitable for manufacturing and scale-up.

The fusion of three targeting modalities led to a significant benefit relative to the use of each method alone. The multitargeted drug-delivery platform resulted in 14% cell viability, whereas the equivalent dosage of free Dox resulted in 81% cell viability. The addition of Herceptin in conjunction with pH-triggered Dox release or NIR ablation increased toxicity relative to that of free Dox but did not cause a decrease in cell viability at the levels reached when all three methods were combined.

In conclusion, we have synthesized a unique multitargeted vehicle that couples three modalities: targeting, triggered release, and thermal ablation. HPG-Dox-30D70H nanoparticles had a high loading efficiency and exhibited pH-responsive Dox release, which was enhanced by laser irradiation. Enhanced targeting relative to that of IgG-labeled nanocarriers was achieved by conjugating Herceptin–PEG conjugates to the surface. Critical to translation, these particles are relatively simple to prepare with high reproducibility. The observed toxicity suggests that multitargeted delivery has great potential as a cancer therapy. HPG-Dox-30D70H is the first carrier to integrate targeting, stimuli-responsive drug delivery, and thermal ablation for use in breast-cancer research.

Received: December 7, 2012
Revised: February 5, 2013
Published online: March 11, 2013

Keywords: cancer nanotechnology · drug delivery · gold nanoparticles · photothermal therapy · pH-sensitive nanoparticles

[1] C. Catzavelos, N. Bhattacharya, Y. C. Ung, J. A. Wilson, L. Roncari, C. Sandhu, P. Shaw, H. Yeger, I. Morava-Protzner, L. Kapusta, E. Franssen, K. I. Pritchard, J. M. Slingerland, *Nat. Med.* **1997**, *3*, 227.
[2] http://www.umm.edu/patiented/articles/how_serious_breast_cancer_000006_6.htm (accessed on September 27, 2012).

[3] Z. Poon, S. Chen, A. C. Engler, H. I. Lee, E. Atas, G. von Maltzahn, S. N. Bhatia, P. T. Hammond, *Angew. Chem.* **2010**, *122*, 7424; *Angew. Chem. Int. Ed.* **2010**, *49*, 7266.
[4] A. Ottaiano, A. di Palma, M. Napolitano, C. Pisano, S. Pignata, F. Tatangelo, G. Botti, A. M. Acquaviva, G. Castello, P. A. Ascierto, R. V. Iaffaioli, S. Scala, *Cancer Immunol. Immunother.* **2005**, *54*, 781.
[5] J. Baselga, L. Norton, J. Albanell, Y. M. Kim, J. Mendelsohn, *Cancer Res.* **1998**, *58*, 2825.
[6] J. O. You, D. T. Auguste, *Biomaterials* **2008**, *29*, 1950.
[7] a) H. K. Moon, S. H. Lee, H. C. Choi, *ACS Nano* **2009**, *3*, 3707; b) J. W. Fisher, S. Sarkar, C. F. Buchanan, C. S. Szot, J. Whitney, H. C. Hatcher, S. V. Torti, C. G. Rylander, M. N. Rylander, *Cancer Res.* **2010**, *70*, 9855.
[8] a) X. H. Huang, P. K. Jain, I. H. El-Sayed, M. A. El-Sayed, *Lasers Med. Sci.* **2008**, *23*, 217; b) V. P. Zharov, K. E. Mercer, E. N. Galitovskaya, M. S. Smeltzer, *Biophys. J.* **2006**, *90*, 619.
[9] H. Yuan, A. M. Fales, T. Vo-Dinh, *J. Am. Chem. Soc.* **2012**, *134*, 11358.
[10] a) L. R. Hirsch, R. J. Stafford, J. A. Bankson, S. R. Sershen, B. Rivera, R. E. Price, J. D. Hazle, N. J. Halas, J. L. West, *Proc. Natl. Acad. Sci. USA* **2003**, *100*, 13549; b) J. Y. Chen, D. L. Wang, J. F. Xi, L. Au, A. Siekkinen, A. Warsen, Z. Y. Li, H. Zhang, Y. N. Xia, X. D. Li, *Nano Lett.* **2007**, *7*, 1318.
[11] S. Y. Liu, Z. S. Liang, F. Gao, S. F. Luo, G. Q. Lu, *J. Mater. Sci. Mater. Med.* **2010**, *21*, 665.
[12] W. X. Chen, R. Bardhan, M. Bartels, C. Perez-Torres, R. G. Pautler, N. J. Halas, A. Joshi, *Mol. Cancer Ther.* **2010**, *9*, 1028.
[13] a) S. M. Lee, H. Park, J. W. Choi, Y. N. Park, C. O. Yun, K. H. Yoo, *Angew. Chem.* **2011**, *123*, 7723; *Angew. Chem. Int. Ed.* **2011**, *50*, 7581; b) J. Z. Du, T. M. Sun, W. J. Song, J. Wu, J. Wang, *Angew. Chem.* **2010**, *122*, 3703; *Angew. Chem. Int. Ed.* **2010**, *49*, 3621.
[14] J. H. Park, G. von Maltzahn, L. L. Ong, A. Centrone, T. A. Hatton, E. Ruoslahti, S. N. Bhatia, M. J. Sailor, *Adv. Mater.* **2010**, *22*, 880.
[15] a) J. O. You, D. T. Auguste, *Nano Lett.* **2009**, *9*, 4467; b) J. O. You, D. T. Auguste, *Biomaterials* **2010**, *31*, 6859.
[16] a) Y. Z. You, D. S. Manickam, Q. H. Zhou, D. Oupicky, *J. Controlled Release* **2007**, *122*, 217; b) J. O. You, D. T. Auguste, *Langmuir* **2010**, *26*, 4607.
[17] R. Hong, G. Han, J. M. Fernández, B. J. Kim, N. S. Forbes, V. M. Rotello, *J. Am. Chem. Soc.* **2006**, *128*, 1078.
[18] a) J. Baselga, *Eur. J. Cancer* **2001**, *37*, 18; b) D. W. Miles, *Breast Cancer Res.* **2001**, *3*, 380.
[19] V. P. Torchilin, *Pharm. Res.* **2007**, *24*, 1.
[20] M. Caldorera-Moore, M. K. Kang, Z. Moore, V. Singh, S. V. Sreenivasan, L. Shi, R. Huang, K. Roy, *Soft Matter* **2011**, *7*, 2879.
[21] N. Dos Santos, K. A. Cox, C. A. McKenzie, F. van Baarda, R. C. Gallagher, G. Karlsson, K. Edwards, L. D. Mayer, C. Allen, M. B. Bally, *Biochim. Biophys. Acta Biomembr.* **2004**, *1661*, 47.
[22] J. Yang, J. Lee, J. Kang, S. J. Oh, H. J. Ko, J. H. Son, K. Lee, J. S. Suh, Y. M. Huh, S. Haam, *Adv. Mater.* **2009**, *21*, 4339.
[23] C. H. Lee, S. H. Cheng, I. P. Huang, J. S. Souris, C. S. Yang, C. Y. Mou, L. W. Lo, *Angew. Chem.* **2010**, *122*, 8390; *Angew. Chem. Int. Ed.* **2010**, *49*, 8214.
[24] H. Wartlick, K. Michaelis, S. Balthasar, K. Strebhardt, J. Kreuter, K. Langer, *J. Drug Targeting* **2004**, *12*, 461.
[25] J. H. Park, G. von Maltzahn, M. J. Xu, V. Fogal, V. R. Kotamraju, E. Ruoslahti, S. N. Bhatia, M. J. Sailor, *Proc. Natl. Acad. Sci. USA* **2010**, *107*, 981.
[26] M. Shi, K. Ho, A. Keating, M. S. Shoichet, *Adv. Funct. Mater.* **2009**, *19*, 1689.
[27] a) C. Chittasupho, S. X. Xie, A. Baoum, T. Yakovleva, T. J. Siahaan, C. J. Berkland, *Eur. J. Pharm. Sci.* **2009**, *37*, 141; b) T. Betancourt, B. Brown, L. Brannon-Peppas, *Nanomedicine* **2007**, *2*, 219.
[28] a) M. Hrubý, C. Konak, K. Ulbrich, *J. Controlled Release* **2005**, *103*, 137; b) Z. G. Gao, D. H. Lee, D. I. Kim, Y. H. Bae, *J. Drug Targeting* **2005**, *13*, 391.
[29] P. Guo, J. O. You, J. Yang, M. A. Moses, D. T. Auguste, *Biomaterials* **2012**, *33*, 8104.
[30] A. Esnouf, P. A. Wright, J. C. Moore, S. Ahmed, *Acupunct. Electro-Ther. Res.* **2007**, *32*, 81–86.
[31] J. You, R. Zhang, G. Zhang, M. Zhong, Y. Liu, C. S. Van Pelt, D. Liang, W. Wei, A. K. Sood, C. Li, *J. Controlled Release* **2012**, *158*, 319.
[32] C. Loo, A. Lowery, N. Halas, J. West, R. Drezek, *Nano Lett.* **2005**, *5*, 709.

